Interfacial spin polarization and resistance in lateral spin-valves incorporating Bi and BiPb thin films

Jin-Seo Noh, Kyoung-Il Lee, and Wooyoung Lee[a)]
Department of Materials Science and Engineering, Yonsei University, 262 Seongsanno, Seodaemun-gu, Seoul 120-749, Republic of Korea

(Received 25 May 2010; accepted 25 August 2010; published online 18 October 2010)

Electrical spin injection and detection have been investigated at cryogenic temperatures using a lateral spin-valve structure. Either Bi or BiPb was used as a nonmagnetic spin medium, while CoFe and NiFe were employed as the spin injector and spin detector, respectively. A large magnetoresistance signal corresponding to $\Delta R=1.2$ mΩ was detected from the BiPb-based spin-valves. From this result, a large spin diffusion length of 230 μm and a high interfacial spin polarization of 10% were derived. From an independent calculation, it was found that the interfacial spin polarization and the associated spin accumulation are strongly correlated with the interfacial resistance. © *2010 American Institute of Physics*. [doi:10.1063/1.3498802]

I. INTRODUCTION

Spintronics is an alternative information processing paradigm, in which the state of spin degree of freedom is a variable in addition to conventional electric charge. It has long been studied for fundamental understanding of the interaction between spins as well as for practical device applications.[1,2] To better understand spintronics, three aspects of transport should be addressed: spin generation, spin diffusion, and spin detection. Although optical means of spin generation has typically been favored,[3] electrical spin injection is considered a better technique for device applications.[4–6] In this process, spin-polarized electrons are expected to come across a ferromagnet/nonferromagnet (F/N) interface and a nonequilibrium population of spins (a spin accumulation) develops in N. Spin relaxation in N occurs mainly by spin-flip scattering related to spin-orbit interaction. Spin detection is a process to sense a voltage (or resistance) at the N/F interface that is proportional to the spin accumulation, using a second proximal ferromagnetic electrode. This whole process was well demonstrated by a Datta–Das spin field-effect transistor (spin FET).[7] Similar to the spin FET, a ferromagnetic metal is used as the electrical spin injector. The injector is conventionally fabricated on narrow band-gap semiconductors such as GaAs (Ref. 8) and AlGaAs (Refs. 5 and 9) due to their long spin lifetime and long carrier mean free path. Spin detection is more challenging. For the reliable spin detection, a lateral nonlocal (LNL) geometry, where a second ferromagnetic electrode is placed in the same plane as the spin injector, is widely exploited. This geometry can eliminate contributions from anisotropic magnetoresistance (AMR) and Hall effects.[10] In order to realize a spintronic device with good characteristics, materials and geometry must be chosen properly.

A material with a long spin diffusion length is desirable because injected spins should survive until they reach a proximal detector. Furthermore, its interface with a F should have a low spin-flip parameter α, where the spin-flip probability S is expressed as $S=1-e^{-\alpha}$.[11] Bismuth (Bi) is a semimetal with a highly anisotropic Fermi surface and unusual transport properties.[12,13] Its intriguing transport properties are attributed to a very small electron effective mass of $m^* \approx 0.001 m_o$, a long carrier mean free path, $\lambda \approx 1.35$ μm, and low carrier concentrations, $n \approx p \approx 3 \times 10^{17}$ cm^{-3}.[14,15] Furthermore, the properties of Bi can be altered by alloying with small concentration of other elements such as Sb[16] and Pb.[17] In this study, we investigated spin injection and spin transport properties in semimetallic Bi and lightly Pb-doped Bi alloy ($Bi_{0.95}Pb_{0.05}$) thin films, using the LNL spin-valve geometry mentioned above. Material-dependent MR signals are presented and discussed with regard to interfacial spin polarization P and interfacial resistance RA. We also derive a large spin diffusion length observed in a BiPb alloy $l_{s,BiPb} \approx 230$ μm. Simulation clarifies the correlation between P and RA.

II. EXPERIMENTAL DETAILS

Figure 1 shows a schematic, perspective view of a lateral spin-valve structure fabricated for this study. First, 25-nm-thick $Co_{0.84}Fe_{0.16}$ (F1) and $Ni_{0.81}Fe_{0.19}$ (F2) films were depos-

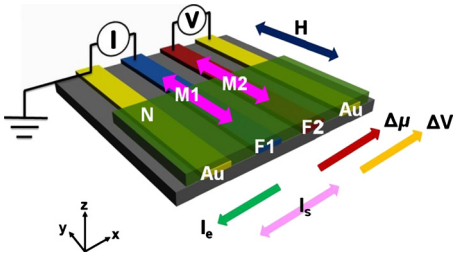

FIG. 1. (Color online) Schematic illustration of a lateral spin-valve structure. F1, F2, and N denote a CoFe spin injector, a NiFe spin detector, and a Bi or BiPb spin medium, respectively. Spin-polarized current (I_s) generates an electrochemical potential difference $\Delta\mu$ that depends on the magnetization orientation of F2. Nonpolarized current (I_e) sinks to ground through the left Au electrode. The nonlocal voltage (ΔV) is measured between F2 and the right Au electrode when dc current is injected at F1. A magnetic field is swept along the magnetic easy axis $\hat{y}$ in order to change the relative magnetization orientations **M1** and **M2**.

a)Electronic mail: wooyoung@yonsei.ac.kr.

ited and patterned on a SiO_2 substrate by a combination of dc magnetron sputtering and a lift-off process. The patterned F1 and F2 electrodes were 10 μm wide. Any oxides on the surfaces of F1 and F2 were removed by Ar^+ plasma etching before deposition of N metals. Either a Bi or $Bi_{0.95}Pb_{0.05}$ film, 9 μm in thickness, was deposited by rf magnetron sputtering and patterned into a bar with width of 0.5 mm and length of 5 mm using a lift-off process. In this structure, F1 and F2 act as a spin injector and a spin detector, respectively, and the distance between the two is varied by using multiple F2 electrodes at a variety of spacing L from F1. F2 is connected to a voltmeter, while injector F1 is connected to a current source. This geometry is called "nonlocal" because the current and voltage circuits are separated, thereby minimizing parasitic contributions such as AMR and Hall effects.

We intentionally employed different ferromagnetic materials with different coercivities ($H_{c,\mathrm{CoFe}} > 100$ Oe, $H_{c,\mathrm{NiFe}} < 30$ Oe), to facilitate the control of relative magnetization states **M1** and **M2**. The magnetic easy axis is aligned along $\hat{y}$ because of shape anisotropy, and an external magnetic field **H** is swept along $\hat{y}$ as well. Spin-polarized carriers are injected from F1 into N across the F1/N interface and generate a nonequilibrium spin accumulation in N. The spin accumulation diffuses radially from the injection point while the nonpolarized bias current (I_e) flows to the left Au electrode. The spin-dependent electrochemical potential difference $\Delta\mu$ is measured as a voltage change ΔV at the opposite Au electrode. Since the voltage change ΔV (and resistance change ΔR) is dependent on the magnetizations **M1** and **M2**, this measurement records MR variation as a function of an in-plane magnetic field. The magnetic field was swept over the range, +800–(–800) Oe. Recently, Dash *et al.*[18] have demonstrated electrical spin injection into silicon at room temperature. Despite this inspiring report, we performed all the measurements in the cryogenic temperature range of 2–10 K to avoid spin relaxation activating at elevated temperatures. This is because the resistivities and lattice vibrations of Bi and Bi-based alloys rapidly increase with increasing temperature.

III. RESULTS AND DISCUSSION

We clearly observed MR behaviors in both Bi and BiPb alloy samples. Figure 2 exhibits representative data for a lateral spin-valve incorporating BiPb as the N metal. In this figure, the two characteristic switching dips are displayed by open symbols: circles (sweep-up) and squares (sweep-down). The distance between F1 and F2 was 30 μm. Beginning at $H_y = -300$ Oe, the spin-valve initially has parallel magnetizations **M1**$\uparrow\uparrow$**M2**. With increasing H_y, **M2** changes its orientation at $H_y = 30-70$ Oe ($H_{c,\mathrm{NiFe}}$), resulting in the antiparallel configuration **M1**$\uparrow\downarrow$**M2** (refer to Fig. 2, right inset).

This magnetization reversal in F2 is accompanied by a significant resistance change, $\Delta R = 1.2$ mΩ. When H_y increases further, **M1** reverses at $H_y = 120-180$ Oe ($H_{c,\mathrm{CoFe}}$), restoring a parallel magnetization configuration. This MR behavior is reproduced when H_y is swept downward from positive to negative fields. The humps observed in the dip in the downward field sweep may be attributed to multistep magnetic domain rotation in F1 and local redistribution of accumulated spins.

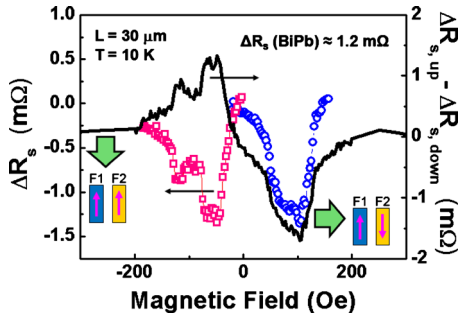

FIG. 2. (Color online) Typical MR behavior obtained from a BiPb-based spin-valve. Open symbols represent ΔR measured on a device with $L = 30$ μm at $T = 10$ K. Upward and downward field sweeps are displayed with blue circles and pink squares, respectively (left hand axis). The solid line shows the difference between up-sweeps and down-sweeps (right hand axis). Insets schematically show the relative magnetization orientations of F1 and F2 before and after resistance change.

The MR associated with spin injection and spin accumulation can be discussed by plotting $\Delta R_{\mathrm{up}} - \Delta R_{\mathrm{down}}$, shown with the solid line (right hand axis) in Fig. 2. Using this plot, we can rule out interruptions from charge current and background contributions which may cause a nonzero sloped baseline. Furthermore, this curve clearly represents the direction of field sweep. It is seen from the solid curve in Fig. 2 that two $\Delta R_{\mathrm{up}} - \Delta R_{\mathrm{down}}$ features occur on either side of $H_y = 0$, with opposite signs, where positive and negative signs represent field sweep-down and sweep-up, respectively. The shape and magnitude of the $\Delta R_{\mathrm{up}} - \Delta R_{\mathrm{down}}$ curve are directly related to those observed in ΔR (Fig. 2, left hand axis). The qualitative MR features were also observed in Bi-based spin-valves. However, the resistance change ΔR was only about 0.1 mΩ, which is about an order of magnitude smaller than the BiPb-based spin-valve. This large difference in ΔR for the two types of spin-valves is related to key materials parameters that control electrical spin injection and accumulation.

Adopting Johnson's charge-spin coupling model,[19] the resistance R_s associated with spin accumulation can be expressed as follows when the spacing L between a spin injector and a detector is smaller than the spin diffusion length, $L \ll l_s$

$$R_s = \frac{P_1 P_2}{e^2} \frac{\tau_s E_F}{1.5\ nV} = P_1 P_2 \frac{\rho l_s^2}{V}, \tag{1}$$

where $P_1(P_2)$ is the spin polarization of F1 (F2) at the interface with N, V is the volume occupied by accumulated spins of δM, and τ_s is the spin relaxation time. The second form in Eq. (1) was derived using an Einstein relation for resistivity and a free electron expression for magnetic susceptibility χ. In the case that $L > l_s$, the spin accumulation decays exponentially as a function of distance L, $\delta M \propto e^{-L/l_s}$, introducing an exponential term

$$R_s = P_1 P_2 \frac{\rho l_s^2}{V} e^{-L/l_s}. \quad (2)$$

We measured R_s using several different F2 electrodes at variable distance L, and a semilogarithmic plot was made for R_s as a function of L. From the slope of this plot, we calculated l_s of the N material, using Eq. (2). The calculated spin diffusion length for the BiPb alloy (refer to Fig. 2) is ~230 μm at 2 K,[17] which is the longest value ever reported for thin films. In comparison, the l_s of Bi appeared to be smaller by a factor of ~3, $l_{s,\mathrm{Bi}} \approx 70$ μm. Assuming radial spin diffusion from a point at the edge of the N, $V \approx \pi l_s^2 d/2$, and substituting this into Eq. (1), $R_s \approx 2P_1P_2\rho/\pi d$. Using $d=9$ μm and the R_s and ρ values measured at 2 K, the product P_1P_2 is calculated as ~0.01, leading to an average spin polarization of two F/BiPb interfaces of $P_{\mathrm{avg}}(\mathrm{BiPb}) \approx 10\%$. A similar calculation for the F/Bi interfaces resulted in $P_{\mathrm{avg}}(\mathrm{Bi}) \approx 0.8\%$. Therefore, it is inferred that the large difference in MR magnitudes, $\Delta R(\mathrm{BiPb})/\Delta R(\mathrm{Bi}) = 12$ for the two N materials, arises mainly from the interfacial spin polarization difference, $P_{\mathrm{avg}}(\mathrm{BiPb})/P_{\mathrm{avg}}(\mathrm{Bi}) \approx 12.5$.

The interfacial spin polarization and the density of spin accumulation also can be affected by the interfacial resistance between F and N. In order to study this effect, we calculated the spin polarization of current crossing the interface and the spin accumulation as a function of interfacial resistance in both Bi and BiPb films, using the extended Valet–Fert model[20] as follows:

$$J_{+(-)} = \frac{1}{e\rho_{+(-)}} \nabla \mu_{+(-)},$$

$$\nabla^2(\mu_+ - \mu_-) = \frac{\mu_+ - \mu_-}{l_s^2}. \quad (3)$$

In the equations above, +(−) refers to spin-up (spin-down), $J_+(J_-)$ is the current density, and $\mu_+(\mu_-)$ is the electrochemical potential for spin +(−). We used spin transport parameters from the literature[11] as well as from our experimental results. These parameters include the bulk resistivity $\rho = 7500$ $\mu\Omega$ cm, 480 $\mu\Omega$ cm, and 5.1 $\mu\Omega$ cm, the bulk spin asymmetry $\beta = 0$, 0, and 0.7, and the spin diffusion length $l_s = 70\,000$ nm, 230 000 nm, and 4.3 nm, all for Bi, BiPb, and NiFe, respectively. The spin accumulation and the associated spin polarization are obtained at a position beneath F1, assuming the interfacial spin asymmetry of $\gamma_{\mathrm{NiFe/N}} = \beta_{\mathrm{NiFe}}$, and taking the product of interfacial resistance R and area A, RA, as a variable.

Figure 3 shows the interfacial spin polarization P as a function of RA. It is apparent that the spin polarization is significantly affected by the interfacial resistance RA, consistent with the issue of conductivity mismatch.[21] The spin polarization rapidly increases with increasing RA until it reaches a plateau at approximately 1×10^{-7} Ω m^2, for both BiPb and Bi. From these calculations, we estimated RA values corresponding to the experimentally measured interfacial spin polarization values ($P_{\mathrm{BiPb}} = 10\%$, $P_{\mathrm{Bi}} = 0.8\%$). As seen in Fig. 3(b), the RA values for BiPb and Bi are approximately 2×10^{-10} Ω m^2 and 1×10^{-10} Ω m^2, respectively.

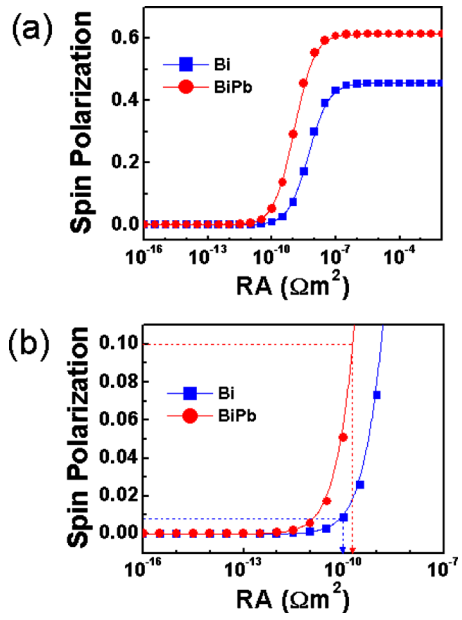

FIG. 3. (Color online) Results of calculation of interfacial spin polarization based on the Valet–Fert model. (a) Interfacial spin polarization vs RA. (b) A magnified view of a portion of (a) for comparison with the experimental values of the interfacial spin polarization. $RA \approx 2 \times 10^{-10}$ Ω m^2 and 1×10^{-10} Ω m^2 correspond to $P_{\mathrm{BiPb}} = 10\%$ and $P_{\mathrm{Bi}} = 0.8\%$, respectively.

Although the difference in RA is merely a factor of two, the interfacial resistance is strongly correlated with the interfacial spin polarization as seen in Fig. 3(a). Figure 3(a) shows that the spin polarization ramp-up begins at $RA \approx 1 \times 10^{-10}$ Ω m^2, which is 2 to 3 orders of magnitude larger than that of a typical F/N metal interface. The combination of highly spin-polarized current and high interfacial resistance led to a large density of spin accumulation δM, from another calculation undertaken in parallel. This is presumably because the high interfacial resistance blocks the backflow of injected spins, as discussed in a previous report.[22] However, the relative magnitudes of δM for BiPb and Bi at a very high RA are not expected to be the same as the difference in P, since $\delta M \propto P \times \rho l_s$ and $\rho(\mathrm{Bi}) \gg \rho(\mathrm{BiPb})$ at low temperature. The measured large value of $\Delta\mu$ (or ΔV) is explained by mutual contributions from a large spin accumulation δM and a low carrier density n, using the relation $\Delta\mu = 2\mu_o \delta M/(3n\mu_B)$, where μ_B is the Bohr magneton and μ_o is the magnetic permeability of free space. These results indicate that a sizable interfacial resistance is essential to relax the large conductivity mismatch and thus to build up electrochemical potential as large as observed from our experimental study.

IV. CONCLUSIONS

We studied two lateral spin-valve structures, employing CoFe as a spin injector, NiFe as a spin detector, and Bi or BiPb as a N spin medium. Electrical spin injection and detection were tested on the spin-valves at low temperatures. Sweeping a magnetic field along the magnetic easy axis, the nonlocal MR was recorded. Clear MR signals were detected from both samples but the magnitude was material-dependent. From an independent calculation, it was found

that the interfacial spin polarization and spin accumulation are large when interfacial resistance is high. We conclude that a large spin accumulation occurs in BiPb because of the high spin polarization and the high resistance at the interfaces. Furthermore, the measured large spin diffusion length implies a low rate of spin-flip scattering in BiPb at low temperatures.

ACKNOWLEDGMENTS

This work was supported by Priority Research Centers Program (Grant No. 2009-0093823) through the National Research Foundation of Korea (NRF), by a grant from the Fundamental R&D Program for Core Technology of Materials funded by the Ministry of Knowledge Economy, and by the Basic Science Research Program (Grant No. NRF-2007-314-C00107) through the National Research Foundation of Korea (NRF).

[1]I. Žutić, J. Fabian, and S. Das Sarma, Rev. Mod. Phys. **76**, 323 (2004).
[2]S. A. Wolf, D. D. Awschalom, R. A. Buhrman, J. M. Daughton, S. von Molnár, M. L. Roukes, A. Y. Chtchelkanova, and D. M. Treger, Science **294**, 1488 (2001).
[3]J. M. Kikkawa, J. A. Gupta, I. Malajovich, and D. D. Awschalom, Physica E (Amsterdam) **9**, 194 (2001).
[4]H. J. Zhu, M. Ramsteer, H. Kostial, M. Wassermeier, H.-P. Schönherr, and K. H. Ploog, Phys. Rev. Lett. **87**, 016601 (2001).
[5]A. T. Hanbicki, B. T. Jonker, G. Itskos, G. Kioseoglou, and A. Petrou, Appl. Phys. Lett. **80**, 1240 (2002).
[6]F. J. Jedema, A. T. Filip, and B. J. van Wees, Nature (London) **410**, 345 (2001).
[7]S. Datta and B. Das, Appl. Phys. Lett. **56**, 665 (1990).
[8]S. A. Crooker, M. Furis, X. Lou, C. Adelmann, D. L. Smith, C. J. Palmstrøm, and P. A. Crowell, Science **309**, 2191 (2005).
[9]K. A. T. Hanbicki, O. M. J. van't Erve, R. Magno, G. Kioseoglou, C. H. Li, B. Jonker, G. Itskos, R. Mallory, M. Yasar, and A. Petrou, Appl. Phys. Lett. **82**, 4092 (2003).
[10]X. Lou, C. Adelmann, S. A. Crooker, E. S. Garlid, J. Zhang, K. S. Madhukar Reddy, S. D. Flexner, C. J. Palmstrøm, and P. A. Crowell, Nat. Phys. **3**, 197 (2007).
[11]J. Bass and W. P. Pratt, Jr., J. Phys.: Condens. Matter **19**, 183201 (2007).
[12]Z. Zhang, X. Sun, M. S. Dresselhaus, J. Y. Ying, and J. Heremans, Phys. Rev. B **61**, 4850 (2000).
[13]Y.-M. Lin, X. Sun, and M. S. Dresselhaus, Phys. Rev. B **62**, 4610 (2000).
[14]J. Heremans and O. P. Hansen, J. Phys. C **12**, 771 (1974).
[15]X. Gonze, J.-P. Michenaud, and J. P. Vigneron, Phys. Scr. **37**, 785 (1988).
[16]A. Ahmad, R. Bilas, and O. P. Katyal, J. Mater. Sci. **30**, 4339 (1995).
[17]K.-I. Lee, J. W. Roh, J. Chang, S.-H. Han, K.-H. Shin, W. Y. Jeung, M. Johnson, and W. Lee, Phys. Rev. B **79**, 195201 (2009).
[18]S. P. Dash, S. Sharma, R. S. Patel, M. P. de Jong, and R. Jansen, Nature (London) **462**, 491 (2009).
[19]M. Johnson, J. Appl. Phys. **75**, 6714 (1994).
[20]T. Valet and A. Fert, Phys. Rev. B **48**, 7099 (1993).
[21]E. I. Rashba, Phys. Rev. B **62**, R16267 (2000).
[22]M. Johnson and J. Byers, Phys. Rev. B **67**, 125112 (2003).